Received: 2 November 2023 | Revised: 26 December 2023 | Accepted: 19 January 2024

https://doi.org/10.1016/j.rpth.2024.102352

ORIGINAL ARTICLE

Human platelets contain a pool of free zinc in dense granules

Walter H. A. Kahr[1,2,3] | Sara J. Henderson[4,5] | Fred G. Pluthero[3] | Harry F. G. Heijnen[6] | Nima Vaezzadeh[4,7] | Alan R. Stafford[8] | James C. Fredenburgh[4,8] | Jeffrey I. Weitz[4,5,7,8]

[1]Division of Haematology/Oncology, Department of Paediatrics, University of Toronto and the Hospital for Sick Children, Toronto, Ontario, Canada

[2]Department of Biochemistry, University of Toronto, Toronto, Ontario, Canada

[3]Cell Biology Program, Research Institute, Hospital for Sick Children, Toronto, Ontario, Canada

[4]Thrombosis and Atherosclerosis Research Institute, McMaster University, Hamilton, Ontario, Canada

[5]Department of Biochemistry and Biomedical Sciences, McMaster University, Hamilton, Ontario, Canada

[6]Departments of Clinical Chemistry and Hematology, University Medical Center Utrecht, Utrecht, The Netherlands

[7]Department of Medical Sciences, McMaster University, Hamilton, Ontario, Canada

[8]Department of Medicine, McMaster University, Hamilton, Ontario, Canada

Correspondence
Walter H.A. Kahr, Departments of Paediatrics & Biochemistry, University of Toronto, Division of Haematology/Oncology, Cell Biology Program, The Hospital for Sick Children, 686 Bay Street, Toronto, ON M5G 0A4, Canada.
Email: walter.kahr@sickkids.ca

Jeffrey I. Weitz, Thrombosis and Atherosclerosis Research Institute, 237 Barton St E, Hamilton, ON L8L 2X2, Canada.
Email: weitzj@taari.ca

Handling Editor: Dr Yotis Senis

Abstract

Background: Activated platelets release procoagulant factors that include Ca^{2+} and Zn^{2+}. Releasable Ca^{2+} stores have been identified in platelet dense granules and the dense tubular system, but similar stores of free Zn^{2+} have not been identified.

Objectives: Guided by studies of platelet Ca^{2+}, we employed minimally disruptive methods to identify and localize concentrated free Zn^{2+} in human platelets.

Methods: Resting platelets from normal donors (NDs), patients with gray platelet syndrome (GPS) lacking α-granules, and patients with Hermansky-Pudlak syndrome (HPS) deficient in dense granules were loaded with cell-permeant fluorescent probes specific to free Ca^{2+} or Zn^{2+}. Ion concentrations were detected in fixed cells as bright puncta via high-resolution confocal microscopy. Ions were also directly detected via transmission electron microscopy and energy dispersive X-ray analysis. Levels of total platelet Ca, Zn, and Mg were measured via inductively coupled plasma optical emission spectroscopy.

Results: Fluorescent Zn^{2+} puncta counts were similar in ND and GPS platelets and markedly lower in HPS platelets, pointing to dense granules as likely reservoirs of free Zn^{2+}. This localization was supported by direct detection of Ca^{2+}, Zn^{2+}, and Na^{+} in platelet dense granules via transmission electron microscopy and energy dispersive X-ray analysis. Measurements of total platelet Ca, Zn, and Mg via inductively coupled plasma optical emission spectroscopy indicated that free Zn^{2+} represents a small proportion of total platelet zinc, consistent with the strong affinity of Zn^{2+} for binding proteins, including several abundant in platelet α-granules.

Conclusion: We conclude that normal human platelets contain a pool of free Zn^{2+} concentrated in dense granules that is available for secretion upon platelet activation and potentially contributes to hemostasis.

KEYWORDS
dense granules, hemostasis, platelets, secretion, zinc

Walter H.A. Kahr and Sara J. Henderson contributed equally to this study.

Essentials

- Platelets initiate and promote hemostasis by secreting the free cations Ca^{2+} and Zn^{2+}.
- Unlike Ca^{2+}, platelet stores of potentially secretable free Zn^{2+} have not been identified.
- We detected Ca^{2+}, Zn^{2+}, and other ions at high resolution within human platelets.
- Comparisons of normal and deficient platelets show that dense granules store concentrated free Zn^{2+}.

1 | INTRODUCTION

Calcium and zinc ions play key roles in many physiological processes [1,2]. Ca^{2+} is an abundant electrolyte in interstitial fluids and blood plasma where the concentration of free Ca^{2+} is roughly equivalent to that bound to albumin and other proteins [1]. In contrast, Zn^{2+} is present at much lower concentrations in plasma (10-20 μM) than Ca^{2+} (>2 mM) and >90% Zn^{2+} ions are bound to albumin and other proteins [3,4], leaving very little free Zn^{2+} in the circulation. Within cells, levels of free Ca^{2+} are typically maintained at submicromolar levels by membrane pumps [1], while intracellular free Zn^{2+} concentrations are very low because of its high affinity to a wide range of proteins [5]. These include enzymes for which Zn^{2+} serves as an essential cofactor [6], and cytosolic metallothioneins [7] that sequester potentially toxic free Zn^{2+} ions [8].

Ca^{2+} and Zn^{2+} play prominent roles in several aspects of hemostasis [4,9]. Both ions are involved in the function of coagulation factors; eg, factor XIII activation [10] requires Ca^{2+} and FXII activation [11] requires Zn^{2+}. Free Ca^{2+} and Zn^{2+} are also involved in platelet adhesion and activation [12,13], where the role of Ca^{2+} has been elucidated over several decades [14]. Ca^{2+} is mobilized both intracellularly and extracellularly during platelet activation [15], and 2 major Ca^{2+} stores have been identified [16]. The primary source of releasable Ca^{2+} is contained in the endomembranous dense tubular system [17] where millimolar Ca^{2+} levels are maintained by sarco(endo)plasmic reticulum Ca^{2+} ATPase (SERCA) 2b. Another pool of Ca^{2+} is maintained in acidic vesicles by SERCA3 acting in concert with a proton gradient driven by vacuolar ATPase [18]. These acidic vesicles include primary lysosomes, which are present in low numbers in human platelets [19], and the more numerous dense granules [20], which also contain adenosine di- and triphosphate, serotonin, and polyphosphate, which contribute to platelet activation, adhesion, and stabilization at sites of vascular damage [21].

Compared with Ca^{2+}, much less is known about the contributions of Zn^{2+} to hemostasis and its interactions with platelets. It has long been known that zinc deficiency is associated with reduced platelet reactivity and bleeding [22], while excess zinc is associated with platelet hyperreactivity [23]. Extracellular release of Zn^{2+} from activated platelets is indicated by the higher levels of Zn^{2+} in serum relative to plasma [24], but unlike Ca^{2+}, potential stores of free Zn^{2+} in platelets have not been conclusively identified. A primary technical challenge in identifying such stores is the high affinity of Zn^{2+} for many platelet proteins, including abundant α-granule cargo such as fibrinogen, albumin, and FXIII [25]. Thus, while studies that localized platelet Zn^{2+} using cell fractionation [26] and tracking with ion-specific reporters [27] detected large amounts of Zn^{2+} within α-granules, most of this is likely to be bound to proteins and thus not mobilizable as free Zn^{2+}.

Guided by studies with Ca^{2+}, the aim of this study was to use established minimally disruptive methods [28–31] to localize concentrated free Zn^{2+} in resting human platelets. The specific goals were to; 1) use ion-specific cell-permeant fluorescent dyes and high-resolution laser fluorescence microscopy [29] to identify sites of concentrated free Zn^{2+} in resting platelets and assess their localization relative to Ca^{2+}; 2) compare normal platelets with those specifically lacking dense or α-granules to gain insights into the intracellular localization of free Zn^{2+}; 3) directly detect concentrations of Zn^{2+} and other ions in normal platelets using transmission electron microscopy and energy dispersive X-ray analysis (TEM-EDX) [32]; and 4) determine the contribution of free Zn^{2+} stores to total platelet zinc.

2 | METHODS

2.1 | Platelet isolation

As per Research Ethics Board approved guidelines and with appropriate informed consent, blood anticoagulated with 3.2% sodium citrate was collected from healthy normal donors (NDs) and from patients diagnosed with hereditary conditions causing deficiency in platelet dense granules (Hermansky-Pudlak syndrome [HPS]) or α-granules (gray platelet syndrome [GPS]). Patients with HPS 1 and 3 carried pathogenic variants of *HSP1*, and the variant of patient 2 was not known; all 3 patients with HPS had <0.6 dense granules per platelet (50 platelets counted) as determined by whole-mount electron microscopy [33]. The patient with GPS had no detectable NBEAL2 expression [34,35]. Platelet-rich plasma (PRP) and washed platelets were prepared as previously described [29].

2.2 | Detection of free Ca^{2+} and Zn^{2+} via high-resolution fluorescence microscopy

Washed platelets were resuspended in Tyrode's buffer (pH 7.2) and live-stained by incubation with varying combinations of the cell-permeant dyes FluoZin-3-AM (5 μM; specific for free Zn^{2+}), Calcium Orange (1 μM; specific for free Ca^{2+}), and MitoTracker Deep Red (specific for mitochondria), all purchased from Life Technologies, with slow rotation following manufacturer instructions. After postincubation in the dark to

allow fluorescent ester cleavage, platelets were hard fixed with 4% paraformaldehyde, rinsed in phosphate buffered saline (PBS), resuspended in PBS+1% bovine serum albumin, and spotted on glass coverslips as previously described [29]. Platelet preparations were poststained with Alexa Fluor–conjugated wheat germ agglutinin (WGA; Life Technologies) to detect sialylated proteins abundant on the platelet surface [30]. Live platelets were not exposed to potentially activating stimuli and were not permeabilized to avoid potential loss of free ion staining. Platelet preparations were mounted and imaged by confocal laser fluorescence microscopy as previously described [29] using emission wavelengths corresponding to FluoZin-3-AM (515 nm), Calcium Orange or WGA-555 (594 nm), and Mitotracker Deep Red or WGA-647 (670 nm). Images were acquired, deconvolved, and registry-corrected using Volocity Analysis (Perkin Elmer), which was also used to visualize images of individual resting platelets (identified by circular shape and discoid XZ profiles) that were manually scored for intracellular puncta. Selected images were exported to Bitplane Imaris 10 for preparation of 3D renders, and high-quality images were exported to Adobe Photoshop or Photoshop Elements for figure preparation. Counts of fluorescent puncta were tabulated with Microsoft Excel and exported to GraphPad Prism for preparation of frequency distribution histograms.

2.3 | Electron microscopy and energy dispersive X-ray analysis

PRP was spotted onto Formvar carbon-covered gold EM grids that were coated with fibrinogen at 4 °C overnight, and then blocked with human serum albumin. After 20 minutes, adherent platelets were fixed with 2% paraformaldehyde and 0.2% glutaraldehyde and rinsed with 0.1M phosphate buffer. Grids were embedded in 1.8% methyl cellulose and adherent platelets were imaged in a beryllium specimen holder (Philips) via TEM with a 200-kV Tecnai 20 microscope (FEI Company) using a LaB6 gun (T20-LaB6). Images were acquired with a 4k × 4k Eagle camera (FEI Company). TEM-EDX analysis [32] was performed to identify elements in nongranular and dense granule areas of adherent platelets mounted using a T20-FEG (field emission gun) equipped with an EDAX CM-200ST X-ray detector. Samples were also subjected to scanning TEM using T20-FEG with a twin objective lens. Data were acquired at an extraction voltage of 4.4 kV, at gun lens setting 6, at a spot size of 6, and with a 70-μm C2 condenser aperture—corresponding to a spot diameter of approximately 1.96 nm. Spot and area spectra for element detection were interpreted using the FEI TEM imaging and analysis software package version 4.8 SP1.

2.4 | Determination of total platelet content of Ca, Mg, and Zn via inductively coupled plasma optical emission spectroscopy

Washed platelets were suspended in PBS at a concentration of 2000/nL, and then diluted at 1:49 in 1.5% tetramethyl ammonium hydroxide and 1.5% HCl to produce lysates with a final concentration equivalent to 40 platelets/nL. Day blank samples were prepared with PBS only. Samples were calibrated against blanks and ion concentration standards and analyzed using a Thermo Scientific iCAP Pro inductively coupled plasma optical emission spectroscopy (ICP-OES) instrument and manufacturer software at the ANALEST facility, University of Toronto. The concentrations (mg/L) of Ca, Mg, and Zn in platelet lysates were determined at 3 different emission lines, and mean values were exported from the analytical software and collated. Tables were prepared using Microsoft Excel. Graphs were prepared using GraphPad Prism software.

3 | RESULTS

3.1 | Detection of concentrated free Ca^{2+} and Zn^{2+} in normal and granule-deficient platelets

The tetramethylrhodamine-based indicator Calcium Orange is a well-established Ca^{2+}-specific intracellular probe that produces a strong signal at wavelengths where scattering and cellular autofluorescence offer little interference [36]. FluoZin-3 has proven similarly useful for probing intracellular Zn^{2+} fluxes in the form of cell-permeant FluoZin-3-AM [37]. Among zinc indicators, FluoZin-3-AM also has the advantage of being relatively insensitive to physiological levels of calcium or magnesium, which can confound detection of free Zn^{2+} [38]. When resting ND platelets were treated with FluoZin-3-AM and/or Calcium Orange prior to fixation, stained with WGA, and imaged by high-resolution confocal laser fluorescence microscopy, intracellular free Zn^{2+} and/or Ca^{2+} were detected as bright puncta within cell boundaries delineated by WGA. Representative images are shown in Figure 1A for ND platelets and platelets from patients with GPS, specifically deficient in α-granules, or from patients with HPS, specifically deficient in dense granules. Some platelets showed bright WGA regions consistent with the open canalicular system, as previously observed [30]. While these platelets were not permeabilized, it is also possible that the contents of α-granules located close to the outer membrane may have been stained with WGA, as is seen in permeabilized cells [29,31]. Diffuse Calcium Orange staining was evident in many platelets, consistent with the high amounts of Ca^{2+} contained in the dense tubular system [16].

Images of individual ND platelets and those from patients with GPS and HPS were scored for intracellular Zn^{2+} puncta (see Methods). The results are summarized as frequency distribution histograms in Figure 1B (data and summary statistics in Table 1). The distributions show that, for all groups, the most frequent score was 0 detectable Zn^{2+} puncta, accounting for 29% to 38% of ND and GPS platelets and 66% to 76% of HPS platelets. The mean Zn^{2+} puncta per platelet ranged from 1.2 to 1.7 for ND (range: 0-8 puncta) and GPS platelets (range: 0-11 puncta), and from 0.3 to 0.5 for HPS platelets (range: 0-4 puncta). These results indicate that while α-granule–deficient platelets had free Zn^{2+} puncta counts comparable to normal platelets, dense granule–deficient platelets had markedly fewer puncta. This

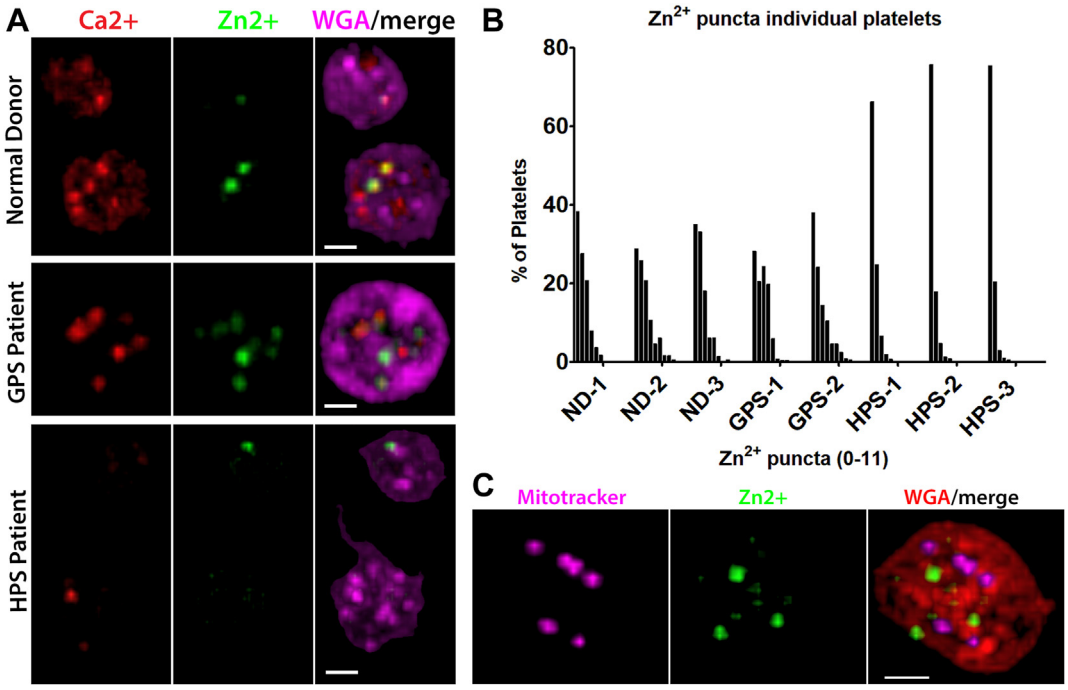

FIGURE 1 Zn^{2+} and Ca^{2+} puncta in normal platelets and cells deficient of alpha or dense granules. (A) Platelets treated with FluoZin-3-AM and Calcium Orange and stained with WGA were imaged by confocal laser fluorescence microscopy to detect puncta indicating concentrated Ca^{2+} (red) or Zn^{2+} (green); WGA (magenta) showed cell membranes and near-membrane structures. Representative resting platelets are shown from a normal donor (top row), patient with alpha granule–deficient GPS (middle row), and patient with dense granule–deficient HPS (bottom row). (B) Similar images were used to score Zn^{2+} puncta in resting platelets ($n > 198$) from 3 NDs (ND-1, ND-2, and ND-3), 2 patients with GPS (GPS-1 and GPS-2), and 3 patients with HPS (HPS-1, HPS-2, and HPS-3); graph shows frequency distributions of counts (left to right from 0 to 11 in each set), which were similar for ND and GPS platelets, and indicated markedly fewer Zn^{2+} puncta in dense granule–deficient platelets (full data in Table 1). (C) Representative images of a normal donor platelet treated with Mitotracker-DR (magenta) and FluoZin3-AM (green) and stained with WGA (red) show Zn^{2+} puncta distinct from mitochondria (data in Table 2). All images are 3D renders of confocal images; bars = 1 μm. GPS, gray platelet syndrome; HPS, Hermansky-Pudlak syndrome; ND, normal donor; WGA, wheat germ agglutinin.

observation points to the dense granules as potential reservoirs of concentrated free Zn^{2+} in human platelets.

3.2 | Overlap of free Zn^{2+} and Ca^{2+} puncta

When platelets were simultaneously stained for both free Zn^{2+} and Ca^{2+}, puncta were often observed to overlap (Figure 1A, top row). This overlap was quantified in 97 ND platelets that contained at least one of each type of punctum. The data summarized in Table 2 show an overlap for 54% (111 of 206) and 47% (111 of 234) of Zn^{2+} and Ca^{2+} puncta, respectively, in these cells. The numbers of puncta per platelet (ie, the ratio of puncta to cells scored) were 2.1 for Zn^{2+} and 2.4 for Ca^{2+}. Both of these values are considerably lower than the estimated mean number of dense granules per platelet reported from studies using electron [39,40] or fluorescence [31,41] microscopy, which ranges from 5 to 8. The most likely reason for this discrepancy is that our method could only detect granules having high concentrations of

TABLE 1 Summary of maximum and mean Zn^{2+} puncta detected in platelets from NDs (n = 2), patients with GPS (n = 2), and patients with HPS (n = 3).

	ND-1	ND-2	ND-3	GPS-1	GPS-2	HPS-1	HPS-2	HPS-3
No. of platelets scored	421	198	381	288	424	800	259	211
Maximum puncta	7	8	7	7	11	4	4	4
Mean puncta	1.18	1.71	1.3	1.60	1.54	0.46	0.34	0.31

Distributions are shown in Figure 2.

Information on race and ethnicity is not available for these subjects and is not likely to be relevant to these findings since GPS and HPS are inherited conditions.

GPS, gray platelet syndrome; HPS, Hermansky-Pudlak syndrome; ND, normal donor.

TABLE 2 Frequencies of overlap of Zn^{2+} puncta with Ca^{2+} puncta or MT in ND platelets containing at least one of each.

	Platelets with Zn^{2+} and Ca^{2+} puncta (n = 97)		
	Zn^{2+}	Ca^{2+}	Zn^{2+} and Ca^{2+}
Total puncta	206	234	111
% overlapped	53.9	47.4	
Puncta/cell	2.1	2.4	1.1
	Platelets with MT and Zn^{2+} puncta (n = 56)		
	Zn^{2+}	MT	Zn^{2+} and MT
Total puncta	115	317	9
% overlapped	7.8	2.8	
Puncta/cell	2.1	5.7	0.2

MT, mitochondria; ND, normal donor.

free Zn^{2+} and/or Ca^{2+} at the time the platelets were loaded and/or imaged. This would explain why many platelets showed no detectable puncta for one or both ions (Figure 1B). While it may also be possible that dense granules differentially accumulate free Zn^{2+} and/or Ca^{2+}, it is likely that fluorescence staining lacks the sensitivity to make a definitive assessment.

3.3 | Free Zn^{2+} in platelet mitochondria

Zn^{2+} and Ca^{2+} fluxes are critical to mitochondrial function [42,43], and human platelets typically contain several mitochondria [39]. The possibility that platelet mitochondria contain detectable concentrations of free Zn^{2+} was examined by imaging ND platelets that were simultaneously treated with FluoZn-3-AM and Mitotracker-DR. We observed 575 mitochondria in a total of 109 platelets (mean = 5.3/cell; range: 1-12), and the results (Figure 1C) indicated that mitochondria were distinct from Zn^{2+} puncta. When 56 platelets containing at least one of each type of punctum were scored, the data (Table 2) revealed overlap for 7.8% of Zn^{2+} puncta and 2.8% of mitochondria. These results suggest that platelet mitochondria may contain a small proportion of free Zn^{2+}.

3.4 | Detection of concentrated Zn^{2+} and Ca^{2+} in dense granules via TEM-EDX

An ideal approach for localizing platelet granules and/or their contents is to use specific antibodies or stains (eg, WGA) that allow their identification via fluorescence microscopy [31]. However, since this approach requires cells to be permeabilized to allow antibodies to enter, it is not useful for localizing ions like Zn^{2+} and Ca^{2+} that can easily escape from permeabilized granules or cells. Platelet dense granules were originally detected as electron dense bodies under whole-mount TEM [44], and concentrated calcium and phosphorus were localized to platelet dense granules in 1974 using a combination of TEM, microincineration, and X-ray spectroscopy [45]. In an effort to extend these findings, we employed a less destructive approach to perform a similar analysis of platelet dense granule contents. TEM imaging was used to identify dense granules against nongranular (ie, background) areas in adherent platelets (Figure 2A, right). Both regions were also subjected to EDX analysis [32], which can detect a wide range of ions and elements. Analysis of individual dense granules detected above-background peaks for C, P, O, Na^{+}, Ca^{2+}, and Zn^{2+} (representative data shown in Figure 2A [left]). Scanning TEM element mapping was used to visualize the presence of Ca^{2+}, Zn^{2+}, Na^{+}, and P, and the results (Figure 2B) confirmed their concentration within individual dense granules.

3.5 | Free Zn^{2+} contribution to total platelet zinc

ICP-OES analysis was used to compare the mean concentrations of elemental Zn, Mg, and Ca in lysates of platelets from 4 ND and 3 HPS patients. The results (Figure 2C) show expected low levels of Ca^{2+} in lysates of dense granule–deficient platelets compared with lysates of normal platelets, while there were no apparent differences in the levels of Zn or Mg. Mean levels of Ca, Zn, and Mg in lysates from ND platelets were 7.1, 0.4, and 2.0 mg/10^{12} platelets, respectively, which are comparable with the results of 6.3, 0.3, and 1.9 mg/10^{12} platelets, respectively, reported from atomic absorption spectroscopy analysis [26]. These results indicate that while free Ca^{2+} in dense granules accounts for a major portion of total calcium present in normal platelets, the free Zn^{2+} in dense granules represents only a small fraction of total platelet zinc. The dense granule store, however, likely represents the main reservoir of releasable free Zn^{2+}.

4 | DISCUSSION

Our observations indicate that concentrated free Zn^{2+} and Ca^{2+} can be detected as discrete puncta in human platelets via fluorescence microscopy (Figure 1A), and the small numbers observed are consistent with the localization of free Zn^{2+} to low-abundance vesicles such as dense granules. This localization is consistent with the much lower frequency of puncta observed in dense granule–deficient HPS platelets, but not in GPS cells lacking α-granules (Figure 1B and Table 1). The substantial overlap observed between Zn^{2+} and Ca^{2+} puncta in normal platelets (Table 2) also points to dense granules as the likely reservoir of free Zn^{2+} in human platelets, a conclusion supported by the direct detection via TEM-EDX of concentrated Zn^{2+}, Ca^{2+}, and other ions within dense granules (Figure 2A, B). Our ICP-OES measurements indicate that free Zn^{2+} in dense granules represents a small portion of total platelet zinc (Figure 2C). This is consistent with the potential toxicity of free Zn^{2+} [46], and also with its strong binding affinity for a wide variety of proteins, including several packaged in α-granules [25].

Our study has some parallels with a recent report by Gotru et al. [27], which examined several aspects of Zn^{2+} homeostasis in human

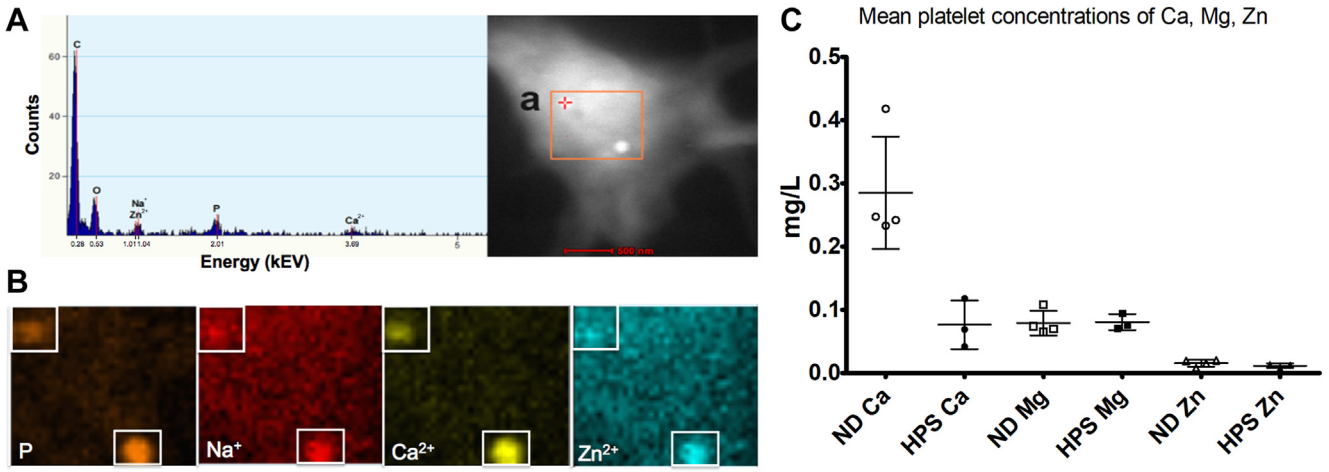

FIGURE 2 Direct detection of Zn^{2+} and Ca^{2+} in normal platelet dense granules and measurement of total platelet Ca, Mg, and Zn in normal and dense granule–deficient platelets. (A) TEM-EDX was performed to identify ions and elements present in dense granules and nongranular regions of adherent normal donor platelets. TEM negative image of a single platelet (right) shows a region (a, orange box) containing 2 dense granules detected as white spots; the EDX spectrum (left) of the granule indicated by the red crosshair shows above-background peaks for carbon (C), oxygen (O), Zn^{2+}, Na^{+}, P, and Ca^{2+}. (B) The entire region was subjected to scanning element mapping, which confirmed the presence of above-background concentrations of P, Na^{+}, Ca^{2+}, and Zn^{2+} in dense granules (white boxes). (C) ICP-OES was used to measure total elemental Ca, Mg, and Zn concentrations (mg/L) in platelet lysates from NDs (n = 4) and patients with dense granule–deficient HPS (n = 3). Results indicate a large Ca deficit in HPS platelets relative to normal, little difference in Mg or Zn levels (bars = mean and SD). Expressed relative to cell number, the mean Ca, Zn, and Mg concentrations in ND platelets were 7.1, 0.4, and 2.0 mg/10^{12} platelets, respectively. HPS, Hermansky-Pudlak syndrome; ICP-OES, inductively coupled plasma optical emission spectroscopy; ND, normal donor; TEM-EDX, transmission electron microscopy with energy dispersive X-ray analysis.

platelets, murine platelets, and megakaryocytes. These studies, however, have clear differences in their aims, approaches, and findings. Salient differences include the following: 1) our principal goal was to definitively localize potentially releasable free Zn^{2+} in resting human platelets, which was a relatively minor aspect of the more widely ranging study of Gotru et al. [27]; 2) while both studies reported observing Zn^{2+} puncta in resting human platelets, they were counted only in our study; 3) only our study examined platelet Ca^{2+} and mitochondria; 4) we exclusively examined human platelets from normal controls and patients deficient in dense or alpha granules, while the other study primarily compared deficient mouse strains and presented limited patient data in supplementary material; 5) we directly localized Zn^{2+} to dense granules via TEM-EDX analysis and quantified total platelet zinc via ICP-OES, while the other study relied primarily on fluorescence microscopy and fluorometric analysis of zinc release from activated platelets; and 6) unlike Gotru et al. [27], we examined neither bound Zn^{2+} in platelets or megakaryocytes nor the effects of Zn^{2+} released from activated platelets on fibrin formation. From these comparisons, we consider our study to be definitive in identifying dense granules as primary reservoirs of free Zn^{2+} in human platelets, consistent with these granules carrying only small molecules and ions.

Although ion release was not directly assessed in this study, we consider it likely that the stores of free Ca^{2+} and Zn^{2+} in dense granules are simultaneously released when platelets are activated. Intracellular and extracellular mobilization are both likely to be highly localized, and for free Zn^{2+}, this release is expected to be physiologically significant given the very low levels of free ion normally present in the cytosol and blood [12]. It has been reported that localized concentrations of free Zn^{2+} of up to 30 μM are possible in the vicinity of activated platelets, which would be sufficient to initiate coagulation by facilitating the binding of FXII and FXI to endothelial cells [47]. Mobilized free Zn^{2+} may also contribute to platelet activation by serving as an extracellular agonist [48] or an intracellular second messenger [49]. Thus, while the amount of free Zn^{2+} stored in platelet dense granules is small, its mobilization may be important for platelet function and hemostasis [4,9,50].

Our findings raise questions concerning how, when, and why free Zn^{2+} is loaded into platelet dense granules. While there appear to be no clear answers at present, some clues may lie in recent reports that the Zn^{2+} transporter transmembrane protein (TMEM) 163 is required for the production of dense granules by megakaryocytes, as well as for platelet dense granule secretion [51]. This may indicate that Zn^{2+} loading facilitates one of more of dense granule development, stability, and function. That loading may be a complex process, since TMEM163 is 1 of over 20 different Zn^{2+} transporters expressed in human cells [52], and 1 of at least 5 expressed in platelets [53]. Clearly, there is much more to be learned about the physiology of platelet-borne free Zn^{2+} and its potential therapeutic relevance.

FUNDING

J.I.W. holds the Heart and Stroke Foundation J. Fraser Mustard Endowed Chair in Cardiovascular Research and Canadian Institutes of Health Research (CIHR) Chair (Tier 1) in Thrombosis. W.H.A.K. is supported by CIHR grants (PJT-153168, PJT-156095).

ETHICS STATEMENT

As per Research Ethics Board approved guidelines at the Hospital for Sick Children and with appropriate informed consent, patients were recruited.

AUTHOR CONTRIBUTIONS

F.G.P. performed fluorescence microscopy imaging (ICP-OES), data analysis, and figure/manuscript preparation. H.F.G.H. performed TEM and energy dispersive X-ray analysis. S.J.H. initiated the study. N.V., A.S., and J.C.F. assisted with study design. W.H.A.K. and J.I.W. contributed to data interpretation and study design.

RELATIONSHIP DISCLOSURE

There are no competing interests to disclose.

REFERENCES

[1] Baird GS. Ionized calcium. *Clin Chim Acta*. 2011;412:696–701.
[2] Hara T, Takeda TA, Takagishi T, Fukue K, Kambe T, Fukada T. Physiological roles of zinc transporters: molecular and genetic importance in zinc homeostasis. *J Physiol Sci*. 2017;67:283–301.
[3] Lu J, Stewart AJ, Sadler PJ, Pinheiro TJ, Blindauer CA. Albumin as a zinc carrier: properties of its high-affinity zinc-binding site. *Biochem Soc Trans*. 2008;36:1317–21.
[4] Vu TT, Fredenburgh JC, Weitz JI. Zinc: an important cofactor in haemostasis and thrombosis. *Thromb Haemost*. 2013;109:421–30.
[5] Andreini C, Bertini I. A bioinformatics view of zinc enzymes. *J Inorg Biochem*. 2012;111:150–6.
[6] Vallee BL, Falchuk KH. The biochemical basis of zinc physiology. *Physiol Rev*. 1993;73:79–118.
[7] Kambe T, Tsuji T, Hashimoto A, Itsumura N. The physiological, biochemical, and molecular roles of zinc transporters in zinc homeostasis and metabolism. *Physiol Rev*. 2015;95:749–84.
[8] Colvin RA, Holmes WR, Fontaine CP, Maret W. Cytosolic zinc buffering and muffling: their role in intracellular zinc homeostasis. *Metallomics*. 2010;2:306–17.
[9] Henderson SJ, Stafford AR, Leslie BA, Kim PY, Vaezzadeh N, Ni R, et al. Zinc delays clot lysis by attenuating plasminogen activation and plasmin-mediated fibrin degradation. *Thromb Haemost*. 2015;113:1278–88.
[10] Singh S, Dodt J, Volkers P, Hethershaw E, Philippou H, Ivaskevicius V, et al. Structure functional insights into calcium binding during the activation of coagulation factor XIII A. *Sci Rep*. 2019;9:11324.
[11] Greengard JS, Griffin JH. Receptors for high molecular weight kininogen on stimulated washed human platelets. *Biochemistry*. 1984;23:6863–9.
[12] Ahmed NS, Lopes-Pires M, Pugh N. Zinc: an endogenous and exogenous regulator of platelet function during hemostasis and thrombosis. *Platelets*. 2021;32:880–7.
[13] Li Z, Delaney MK, O'Brien KA, Du X. Signaling during platelet adhesion and activation. *Arterioscler Thromb Vasc Biol*. 2010;30:2341–9.
[14] Rink TJ, Sage SO. Calcium signaling in human platelets. *Annu Rev Physiol*. 1990;52:431–49.
[15] Hou Y, Carrim N, Wang Y, Gallant RC, Marshall A, Ni H. Platelets in hemostasis and thrombosis: novel mechanisms of fibrinogen-independent platelet aggregation and fibronectin-mediated protein wave of hemostasis. *J Biomed Res*. 2015;29:437–44.
[16] Jardín I, López JJ, Pariente JA, Salido GM, Rosado JA. Intracellular calcium release from human platelets: different messengers for multiple stores. *Trends Cardiovasc Med*. 2008;18:57–61.
[17] Gerrard JM, White JG, Peterson DA. The platelet dense tubular system: its relationship to prostaglandin synthesis and calcium flux. *Thromb Haemost*. 1978;40:224–31.
[18] López JJ, Camello-Almaraz C, Pariente JA, Salido GM, Rosado JA. Ca^{2+} accumulation into acidic organelles mediated by Ca^{2+}- and vacuolar H^{+}-ATPases in human platelets. *Biochem J*. 2005;390:243–52.
[19] Bentfeld-Barker ME, Bainton DF. Identification of primary lysosomes in human megakaryocytes and platelets. *Blood*. 1982;59:472–81.
[20] White JG. The dense bodies of human platelets. Origin of serotonin storage particles from platelet granules. *Am J Pathol*. 1968;53:791–808.
[21] Sharda A, Flaumenhaft R. The life cycle of platelet granules. *F1000Res*. 2018;7:236.
[22] Gordon PR, Woodruff CW, Anderson HL, O'Dell BL. Effect of acute zinc deprivation on plasma zinc and platelet aggregation in adult males. *Am J Clin Nutr*. 1982;35:113–9.
[23] Marx G, Krugliak J, Shaklai M. Nutritional zinc increases platelet reactivity. *Am J Hematol*. 1991;38:161–5.
[24] Chen WJ, Zhao CY, Zheng TL. Comparison of zinc contents in human serum and plasma. *Clin Chim Acta*. 1986;155:185–7.
[25] Marx G, Korner G, Mou X, Gorodetsky R. Packaging zinc, fibrinogen, and factor XIII in platelet alpha-granules. *J Cell Physiol*. 1993;156:437–42.
[26] Makino TK. Ca, Mg, and Zn in platelets, as determined by atomic absorption spectrometry with use of a sealed decomposition bomb and discrete nebulization. *Clin Chem*. 1985;31:609–12.
[27] Kiran Gotru S, van Geffen JP, Nagy M, Mammadova-Bach E, Eilenberger J, Volz J, et al. Defective Zn^{2+} homeostasis in mouse and human platelets with α- and δ-storage pool diseases. *Sci Rep*. 2019;9:8333.
[28] Crescente M, Pluthero FG, Li L, Lo RW, Walsh TG, Schenk MP, et al. Intracellular trafficking, localization, and mobilization of platelet-borne thiol isomerases. *Arterioscler Thromb Vasc Biol*. 2016;36:1164–73.
[29] Pluthero FG, Kahr WHA. Imaging platelets and megakaryocytes by high-resolution laser fluorescence microscopy. *Methods Mol Biol*. 2018;1812:13–31.
[30] Robinson CM, Poon BPK, Kano Y, Pluthero FG, Kahr WHA, Ohh M. A hypoxia-inducible HIF1-GAL3ST1-sulfatide axis enhances ccRCC immune evasion via increased tumor cell-platelet binding. *Mol Cancer Res*. 2019;17:2306–17.
[31] Pluthero FG, Kahr WHA. Evaluation of human platelet granules by structured illumination laser fluorescence microscopy. *Platelets*. 2023;34:2157808.
[32] Scimeca M, Bischetti S, Lamsira HK, Bonfiglio R, Bonanno E. Energy dispersive X-ray (EDX) microanalysis: a powerful tool in biomedical research and diagnosis. *Eur J Histochem*. 2018;62:2841.
[33] Christensen H, Kahr WHA. Diagnosis of platelet disorders by electron microscopy. In: Stirling J, Curry A, Eyden B, eds. *Diagnostic electron microscopy: a practical guide to interpretation and technique*. John Wiley & Sons Ltd; 2012, p. 277–91.
[34] Pluthero FG, Di Paola J, Carcao MD, Kahr WHA. NBEAL2 mutations and bleeding in patients with gray platelet syndrome. *Platelets*. 2018;29:632–5.
[35] Kahr WH, Hinckley J, Li L, Schwertz H, Christensen H, Rowley JW, et al. Mutations in NBEAL2, encoding a BEACH protein, cause gray platelet syndrome. *Nat Genet*. 2011;43:738–40.
[36] Takahashi A, Camacho P, Lechleiter JD, Herman B. Measurement of intracellular calcium. *Physiol Rev*. 1999;79:1089–125.
[37] Muylle FA, Adriaensen D, De Coen W, Timmermans JP, Blust R. Tracing of labile zinc in live fish hepatocytes using FluoZin-3. *Biometals*. 2006;19:437–50.
[38] Zhao J, Bertoglio BA, Gee KR, Kay AR. The zinc indicator FluoZin-3 is not perturbed significantly by physiological levels of calcium or magnesium. *Cell Calcium*. 2008;44:422–6.

[39] Pokrovskaya ID, Yadav S, Rao A, McBride E, Kamykowski JA, Zhang G, et al. 3D ultrastructural analysis of alpha-granule, dense granule, mitochondria, and canalicular system arrangement in resting human platelets. *Res Pract Thromb Haemost*. 2020;4:72–85.

[40] Brunet JG, Iyer JK, Badin MS, Graf L, Moffat KA, Timleck M, et al. Electron microscopy examination of platelet whole mount preparations to quantitate platelet dense granule numbers: implications for diagnosing suspected platelet function disorders due to dense granule deficiency. *Int J Lab Hematol*. 2018;40:400–7.

[41] Westmoreland D, Shaw M, Grimes W, Metcalf DJ, Burden JJ, Gomez K, et al. Super-resolution microscopy as a potential approach to diagnosis of platelet granule disorders. *J Thromb Haemost*. 2016;14:839–49.

[42] Liu HY, Gale JR, Reynolds IJ, Weiss JH, Aizenman E. The multifaceted roles of zinc in neuronal mitochondrial dysfunction. *Biomedicines*. 2021;9:489.

[43] Garbincius JF, Elrod JW. Mitochondrial calcium exchange in physiology and disease. *Physiol Rev*. 2022;102:893–992.

[44] Urban D, Pluthero FG, Christensen H, Baidya S, Rand ML, Das A, et al. Decreased numbers of dense granules in fetal and neonatal platelets. *Haematologica*. 2017;102:e36–8. https://doi.org/10.3324/haematol.2016.152421

[45] Martin JH, Carson FL, Race GJ. Calcium-containing platelet granules. *J Cell Biol*. 1974;60:775–7. https://doi.org/10.1083/jcb.60.3.775

[46] Mammadova-Bach E, Braun A. Zinc homeostasis in platelet-related diseases. *Int J Mol Sci*. 2019;20:5258.

[47] Mahdi F, Shariat-Madar Z, Schmaier AH. The relative priority of prekallikrein and factors XI/XIa assembly on cultured endothelial cells. *J Biol Chem*. 2003;278:43983–90.

[48] Watson BR, White NA, Taylor KA, Howes JM, Malcor JD, Bihan D, et al. Zinc is a transmembrane agonist that induces platelet activation in a tyrosine phosphorylation-dependent manner. *Metallomics*. 2016;8:91–100.

[49] Ahmed NS, Lopes Pires ME, Taylor KA, Pugh N. Agonist-evoked increases in intra-platelet zinc couple to functional responses. *Thromb Haemost*. 2019;119:128–39.

[50] Henderson SJ, Xia J, Wu H, Starfford AR, Leslie BA, Fredenburgh JC, et al. Zinc promotes clot stability by accelerating clot formation and modifying fibrin structure. *Thromb Haemost*. 2016;115:533–42.

[51] Yuan Y, Liu T, Huang X, Chen Y, Zhang W, Li T, et al. A zinc transporter, transmembrane protein 163, is critical for the biogenesis of platelet dense granules. *Blood*. 2021;137:1804–17.

[52] Kambe T, Taylor KM, Fu D. Zinc transporters and their functional integration in mammalian cells. *J Biol Chem*. 2021;296:100320.

[53] Kim MS, Pinto SM, Getnet D, Nirujogi RS, Manda SS, Chaerkady R, et al. A draft map of the human proteome. *Nature*. 2014;509:575–81.